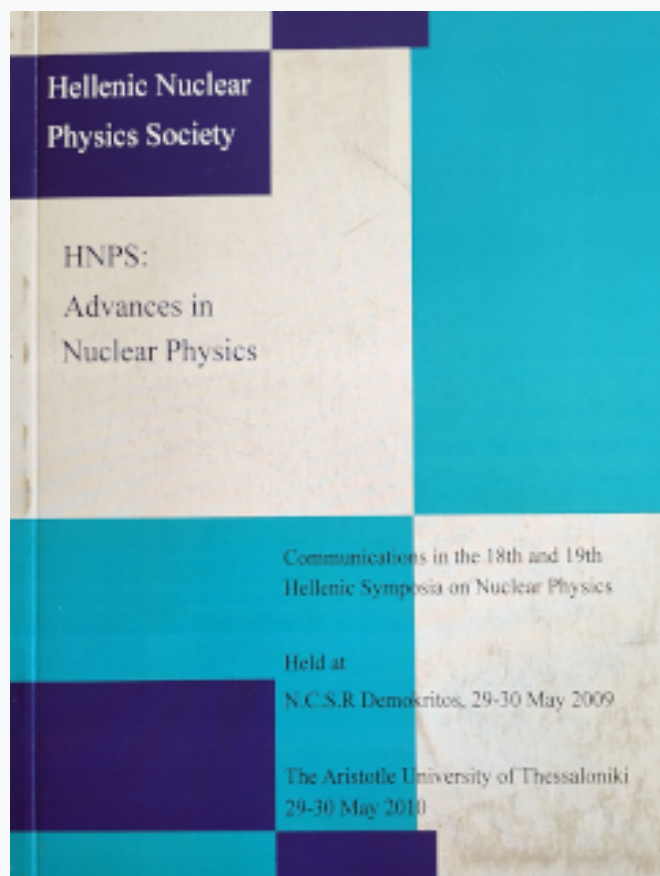


## HNPS Advances in Nuclear Physics

Vol 18 (2010)

HNPS2010



### To cite this article:

Bonatsos, D. (2019). Approximate symmetries in the Interacting Boson Model. *HNPS Advances in Nuclear Physics*, 18, 37-42. <https://doi.org/10.12681/hnps.2536>

# Approximate symmetries in the Interacting Boson Model

Dennis Bonatsos

*Institute of Nuclear Physics, N.C.S.R. “Demokritos”, GR-15310 Aghia Paraskevi, Attiki, Greece*

---

## Abstract

Dynamical symmetries have played a central role for many years in the study of nuclear structure. Recently, the concepts of Partial Dynamical Symmetry (PDS) and Quasi-Dynamical Symmetry (QDS) have been introduced. We shall discuss examples of PDS and QDS appearing in the large boson number limit of the Interacting Boson Model.

---

Dynamical symmetries have been used in nuclear structure for several years. A well known example is provided by the Interacting Boson Model, having an overall  $U(6)$  symmetry, within which the dynamical symmetries  $U(5)$ ,  $SU(3)$ , and  $O(6)$  occur. These dynamical symmetries are traditionally placed at the corners of the symmetry triangle of IBM, depicted in Fig. 3.

More recently, two new kinds of symmetries have been considered, the Partial Dynamical Symmetries (PDS) [1–3] and the Quasi-Dynamical Symmetries (QDS) [4–8].

There are three kinds of Partial Dynamical Symmetries [1–3]:

- i) Type I, where some of the states preserve all the relevant symmetry.
- ii) Type II, in which all the states preserve part of the dynamical symmetry.
- iii) Type III, where some of the states preserve part of the symmetry.

We will show [9] that signs of a yet unknown PDS seem to appear near the critical line [10,11] of the IBM.

On the other hand, Quasi-Dynamical Symmetries [4–8] are defined as the situations in which dynamical symmetries persist despite strong symmetry-breaking interactions. We will show [12] that such a QDS appears to be providing an explanation for the existence of the Alhassid–Whelan arc of regularity [13,14] among chaotic regions within the symmetry triangle of the IBM.

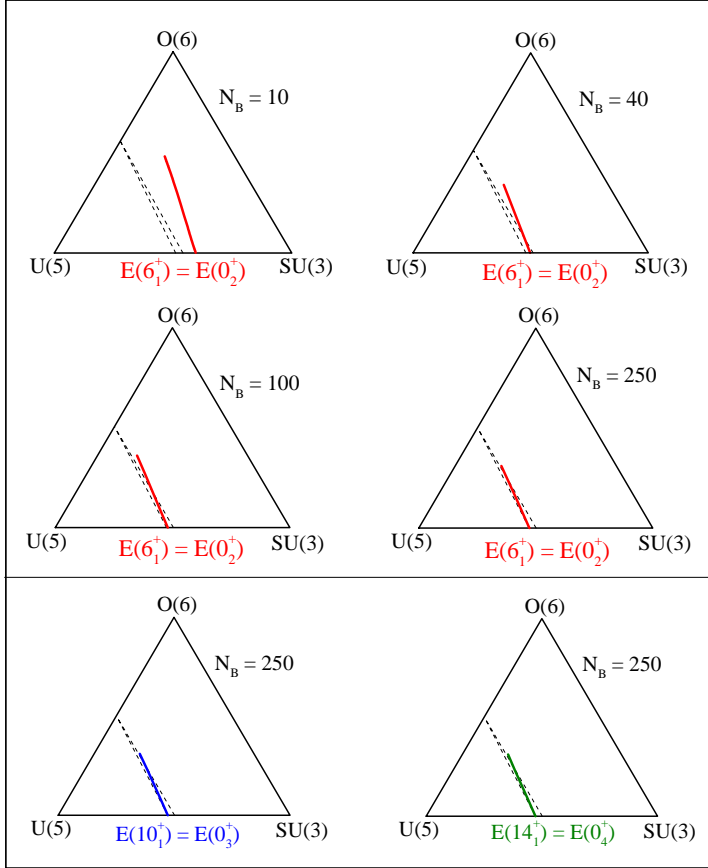


Fig. 1. (Top) Line of degeneracy between the  $0_2^+$  and  $6_1^+$  levels (solid line) for  $N_B = 10, 40, 100$ , and  $250$  in the IBA triangle. (Bottom) Line of degeneracy between the  $0_3^+$  and  $10_1^+$  levels (solid line) for  $N_B = 250$  (left) and between the  $0_4^+$  and  $14_1^+$  levels (solid line) for  $N_B = 250$  (right) in the IBA triangle. The dashed lines denote the critical region in the IBA obtained in the large  $N_B$  limit from the intrinsic state formalism. Taken from Ref. [9].

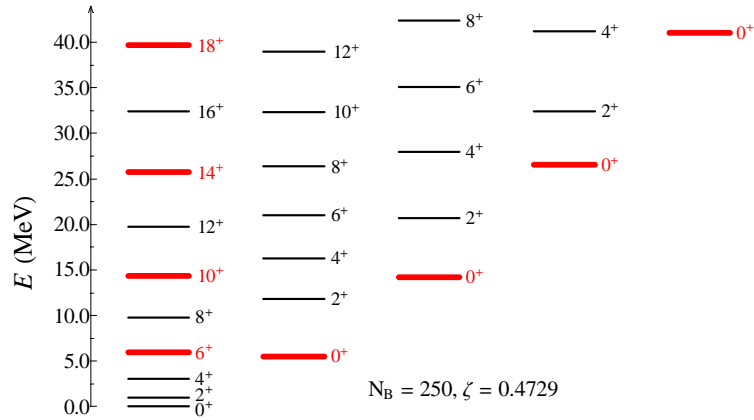


Fig. 2. Energies of low-lying states (normalized to  $E(2_1^+)=1$ ) of the Hamiltonian of Eq. (1) with  $\chi=-\sqrt{7}/2$ ,  $\zeta=0.4729$ , and  $N_B=250$ . The parameter  $\zeta$  was chosen to reproduce the approximate degeneracy of  $E(0_2^+)$  and  $E(6_1^+)$ . Taken from Ref. [9].

$$H(\zeta, \chi) = c \left[ (1 - \zeta) \hat{n}_d - \frac{\zeta}{4N_B} \hat{Q}^\chi \cdot \hat{Q}^\chi \right], \quad (1)$$

where  $\hat{n}_d = d^\dagger \cdot \tilde{d}$ ,  $\hat{Q}^\chi = (s^\dagger \tilde{d} + d^\dagger s) + \chi(d^\dagger \tilde{d})^{(2)}$ ,  $N_B$  is the number of valence bosons, and  $c$  is a scaling factor. Calculations in this work have been performed with the code IBAR [15], which has recently been developed to handle large boson numbers.

As seen in Fig. 1, certain lines representing degeneracies of pairs of levels  $[(6_1, 0_2^+), (10_1, 0_3^+), (14_1, 0_4^+)]$  approach the critical region as the boson number is increased. In Fig. 2 one can see that these are degeneracies between members of the ground state band (gsb) and the  $0^+$  states studied in Refs. [16,17].

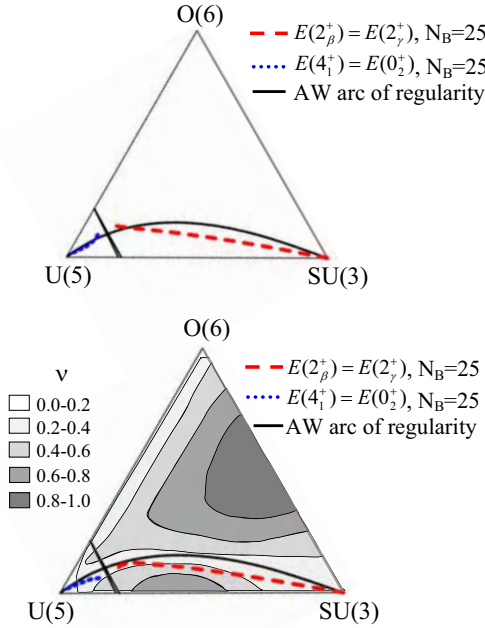


Fig. 3. IBA symmetry triangle in the parametrization of Eq. (2) with the three dynamical symmetries and the Alhassid-Whelan arc of regularity. The shape coexistence region between spherical and deformed phases, shown by slanted lines near the U(5) vertex, encloses a first order phase transition terminating in a point of second order transition on the U(5)-O(6) leg. The loci of the degeneracies  $E(2_\beta^+) = E(2_\gamma^+)$  (dashed line on the right, corresponding to the QDS discussed in the text) and  $E(4_1^+) = E(0_2^+)$  (dotted line on the left) are shown for  $N_B = 250$  (top) and  $N_B = 25$  (bottom). In the bottom part, the  $\nu$ -diagram, based on Ref. [14] is shown. Taken from Ref. [12].

One can see empirically that these states approximately satisfy [17] the expression  $J(J + 2) = 12n(n + 3)$ , where  $J$  indicates the angular momentum of

the gsb members, while  $n$  enumerates the  $0^+$  states. These degeneracies maybe indicate the existence of some underlying symmetry, which is yet unknown. Locating this symmetry could help in clarifying the nature of the X(5) critical point symmetry, which remains unknown to date.

40

Now we turn attention to the QDS concept. A puzzle which has been around for nearly 20 years is the existence of the Alhassid–Whelan arc of regularity [13,14], a region of increased regularity within the symmetry triangle of the IBM, amidst chaotic regions, as shown in Fig. 3. In these studies a different parametrization (using the parameters  $\eta$ ,  $\chi$ ) of the IBM Hamiltonian of Eq. (2) has been used, reading [13,14]

$$H(\eta, \chi) = c \left[ \eta \hat{n}_d + \frac{\eta - 1}{N_B} \hat{Q}^\chi \cdot \hat{Q}^\chi \right], \quad (2)$$

where the symbols have the same meaning as in Eq. (1).

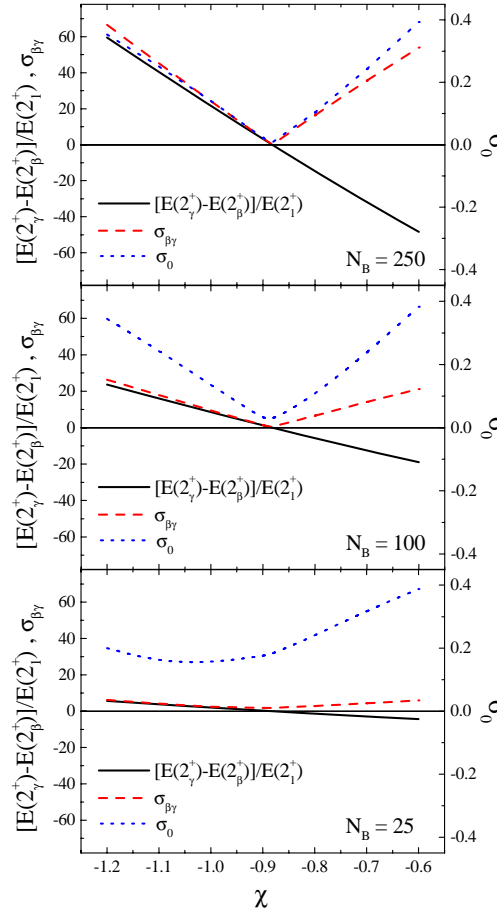


Fig. 4. The energy difference  $E(2_\gamma^+) - E(2_\beta^+)$  (normalized to  $E(2_1^+)$ ) and the quality measures  $\sigma_{\beta\gamma}$  [Eq. (3), up to  $L_{max}=10$ ] and  $\sigma_0$  [Eq. (4), up to  $i_{max}=9$ ], are shown for  $\eta=0.632$ , varying  $\chi$ , and boson numbers  $N_B=25, 100, 250$ . Taken from Ref. [12].

We shall show that an underlying SU(3) QDS is responsible for the existence of the arc. In order to do so, we shall use some measures of SU(3), like the

$$\sigma_{\beta\gamma} = \sqrt{\frac{\sum_{2}^{L_{max}} [E(L_{\beta}^{+}) - E(L_{\gamma}^{+})]^2}{\frac{L_{max}}{2} - 1}}, \quad (3)$$

where  $L_{\beta}^{+}=L_{\gamma}^{+}$  and all energies are normalized to  $E(2_1^{+})$ . In order to examine to which degree the  $0^{+}$  states occurring in an IBM calculation obey the SU(3) rules, we shall also use the relevant rms deviation of the  $0^{+}$  states from the positions predicted by the second order Casimir operator of SU(3) [12],

$$\sigma_0 = \sqrt{\frac{\sum_{3}^{i_{max}} [E(0_i^{+})^{th} - E(0_i^{+})^{SU(3)}]^2}{i_{max} - 3}}. \quad (4)$$

with all energies normalized to  $E(0_2^{+})$  and considering the lowest nine  $0^{+}$  states (i.e.,  $i_{max}=9$ ).

As depicted in Fig. 4, one can see numerically that both measures of SU(3) behaviour exhibit at large boson numbers strong minima at the point where the degeneracy  $2_{\gamma}^{+} = 2_{\beta}^{+}$  occurs. This indicates that the spectra acquire an SU(3) structure if this degeneracy is imposed. In Ref. [9] one can see that the SU(3) degeneracies appear also at higher bands, well beyond the gsb.

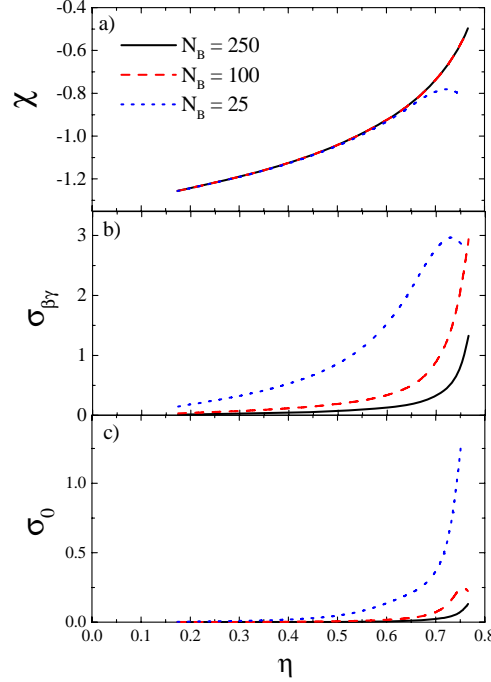


Fig. 5. The  $|\chi|$  parameter values providing the degeneracy  $E(2_{\beta}^{+})=E(2_{\gamma}^{+})$  and the quality measures  $\sigma_{\beta\gamma}$  [Eq. (3), up to  $L_{max}=10$ ] and  $\sigma_0$  [Eq. (4), up to  $i_{max}=9$ ], are shown for different values of  $\eta$  and  $N_B=25, 100, 250$ . Taken from Ref. [9].

The track of this degeneracy within the symmetry triangle of the IBM shown in Fig. 3, nearly coincides with the Alhassid–Whelan arc of regularity, suggest-

ing an underlying SU(3) symmetry as the reason behind the existence of the branch of the arc between the SU(3) vertex and the critical line. In Fig. 5 one can see that the SU(3) measures remain close to their SU(3) values far beyond the SU(3) point, thus providing an example of a SU(3) QDS. A similar line, based on the degeneracy  $E(4_1^+) = E(0_2^+)$ , can be obtained between the U(5) vertex and the critical line, but the relevant minima there are rather shallow, in sharp contrast with the deep minima of Fig. 4.

In conclusion, we have shown some examples of PDS and QDS appearing in the framework of the IBM. Further searches for approximate symmetries in nuclear structure models appear to be promising.

## References

- [1] Y. Alhassid and A. Leviatan, *J. Phys. A: Math. Gen.* **25** (1992) L1265.
- [2] A. Leviatan, *Phys. Rev. Lett.* **77** (1996) 818.
- [3] A. Leviatan and P. Van Isacker, *Phys. Rev. Lett.* **89** (2002) 222501.
- [4] D. J. Rowe, *Phys. Rev. Lett.* **93** (2004) 122502.
- [5] D. J. Rowe, P. S. Turner, and G. Rosensteel, *Phys. Rev. Lett.* **93** (2004) 232502.
- [6] D. J. Rowe, *Nucl. Phys. A* **745** (2004) 47.
- [7] P. S. Turner and D. J. Rowe, *Nucl. Phys. A* **756** (2005) 333.
- [8] G. Rosensteel and D. J. Rowe, *Nucl. Phys. A* **759** (2005) 92.
- [9] D. Bonatsos, E.A. McCutchan, R.F. Casten, and R.J. Casperson, *Phys. Rev. Lett.* **100** (2008) 142501.
- [10] F. Iachello, N. V. Zamfir, and R. F. Casten, *Phys. Rev. Lett.* **81** (1998) 1191.
- [11] E. A. McCutchan, D. Bonatsos, and N. V. Zamfir, *Phys. Rev. C* **74** (2006) 034306.
- [12] D. Bonatsos, E. A. McCutchan, and R. F. Casten, *Phys. Rev. Lett.* **104** (2010) 022502.
- [13] Y. Alhassid and N. Whelan, *Phys. Rev. Lett.* **67** (1991) 816.
- [14] N. Whelan and Y. Alhassid, *Nucl. Phys. A* **556** (1993) 42.
- [15] R. J. Casperson, Ph.D. thesis, Yale University (2010).
- [16] D. Bonatsos, E.A. McCutchan, and R.F. Casten, *Phys. Rev. Lett.* **101** (2008) 022501.
- [17] D. Bonatsos, E.A. McCutchan, R.F. Casten, R.J. Casperson, V. Werner, and E. Williams, *Phys. Rev. C* **80** (2009) 034311.